Research Article | Vol. 26, No. 16 | 6 Aug 2018 | OPTICS EXPRESS 20861
Optics EXPRESS

Compositionally controlled plasmonics in amorphous semiconductor metasurfaces

DAVIDE PICCINOTTI,[1,4] BEHRAD GHOLIPOUR,[1,2,4,*] JIN YAO,[2] KEVIN F. MACDONALD,[1] BRIAN E. HAYDEN,[2] AND NIKOLAY I. ZHELUDEV[1,3]

[1]*Optoelectronics Research Centre and Centre for Photonic Metamaterials, University of Southampton, Southampton SO17 1BJ, UK*
[2]*Department of Chemistry, University of Southampton, Southampton SO17 1BJ, UK*
[3]*Centre for Disruptive Photonic Technologies, School of Physical and Mathematical Sciences & The Photonics Institute, Nanyang Technological University, 637371, Singapore*
[4]*These authors contributed equally*
[*]*bg305@orc.soton.ac.uk*

Abstract: Amorphous bismuth telluride (Bi:Te) provides a composition-dependent, CMOS-compatible alternative material platform for plasmonics in the ultraviolet-visible spectral range. Thin films of the chalcogenide semiconductor are found, using high-throughput physical vapor deposition and characterization techniques, to exhibit a plasmonic response (a negative value of the real part of relative permittivity) over a band of wavelengths extending from ~250 nm to between 530 and 978 nm, depending on alloy composition (Bi:Te at% ratio). The plasmonic response is illustrated via the fabrication of subwavelength period nano-grating metasurfaces, which present strong, period-dependent plasmonic absorption resonances in the visible range, manifested in the perceived color of the nanostructured domains in reflection.

OCIS codes: (160.3918) Metamaterials; (160.6000) Semiconductor materials; (250.5403) Plasmonics.

References and links

1. M. I. Stockman, K. Kneipp, S. I. Bozhevolnyi, S. Saha, A. Dutta, J. Ndukaife, N. Kinsey, H. Reddy, U. Guler, V. Shalaev, A. Boltasseva, B. Gholipour, H. N. S. Krishnamoorthy, K. F. Macdonald, C. Soci, N. I. Zheludev, V. Savinov, R. Singh, P. Groß, C. Lienau, M. Vadai, M. L. Solomon, D. R. Barton III, M. Lawrence, J. A. Dionne, S. V. Boriskina, R. Esteban, J. Aizpurua, X. Zhang, S. Yang, D. Wang, W. Wang, T. W. Odom, N. F. Van Hulst, and M. Kling, "Roadmap on plasmonics," J. Opt. in press.
2. S. Kruk and Y. Kivshar, "Functional meta-optics and nanophotonics govern by mie resonances," ACS Photonics **4**(11), 2638–2649 (2017).
3. D. Lin, P. Fan, E. Hasman, and M. L. Brongersma, "Dielectric gradient metasurface optical elements," in *Science*(2014), pp. 298–302.
4. G. V. Naik, V. M. Shalaev, and A. Boltasseva, "Alternative plasmonic materials: beyond gold and silver," Adv. Mater. **25**(24), 3264–3294 (2013).
5. P. Moitra, Y. Yang, Z. Anderson, I. I. Kravchenko, D. P. Briggs, and J. Valentine, "Realization of an all-dielectric zero-index optical metamaterial," Nat. Photonics **7**(10), 791–795 (2013).
6. G. V. Naik, J. Kim, and A. Boltasseva, "Oxides and nitrides as alternative plasmonic materials in the optical range," Opt. Mater. Express **1**(6), 1090–1099 (2011).
7. G. V. Naik, J. Liu, A. V. Kildishev, V. M. Shalaev, and A. Boltasseva, "Demonstration of Al:ZnO as a plasmonic component for near-infrared metamaterials," Proc. Natl. Acad. Sci. U.S.A. **109**(23), 8834–8838 (2012).
8. Y. Wang, A. Capretti, and L. Dal Negro, "Wide tuning of the optical and structural properties of alternative plasmonic materials," Opt. Mater. Express **5**(11), 2415–2430 (2015).
9. M. Wuttig, H. Bhaskaran, and T. Taubner, "Phase-change materials for non-volatile photonic applications," Nat. Photonics **11**(8), 465–476 (2017).
10. S. Guerin, B. Hayden, D. W. Hewak, and C. Vian, "Synthesis and screening of phase change chalcogenide thin film materials for data storage," ACS Comb. Sci. **19**(7), 478–491 (2017).
11. K. B. Borisenko, J. Shanmugam, B. A. O. Williams, P. Ewart, B. Gholipour, D. W. Hewak, R. Hussain, T. Jávorfi, G. Siligardi, and A. I. Kirkland, "Photo-induced optical activity in phase-change memory materials," Sci. Rep. **5**(1), 8770 (2015).

#325785 https://doi.org/10.1364/OE.26.020861
Journal © 2018 Received 9 Mar 2018; revised 25 May 2018; accepted 1 Jun 2018; published 31 Jul 2018

Optics EXPRESS

12. M. A. Hughes, Y. Fedorenko, B. Gholipour, J. Yao, T. H. Lee, R. M. Gwilliam, K. P. Homewood, S. Hinder, D. W. Hewak, S. R. Elliott, and R. J. Curry, "N-type chalcogenides by ion implantation," Nat. Commun. **5**(1), 5346 (2014).
13. B. Gholipour, C. C. Huang, J. Y. Ou, and D. W. Hewak, "Germanium antimony lateral nanowire phase change memory by chemical vapor deposition," Phys. Status Solidi B. **250**(5), 994–998 (2013).
14. B. Gholipour, J. Zhang, K. F. MacDonald, D. W. Hewak, and N. I. Zheludev, "An all-optical, non-volatile, bidirectional, phase-change meta-switch," Adv. Mater. **25**(22), 3050–3054 (2013).
15. B. Xia, P. Ren, A. Sulaev, P. Liu, S. Q. Shen, and L. Wang, "Indications of surface-dominated transport in single crystalline nanoflake devices of topological insulator bi1.5sb0.5te1.8se1.2," Phys. Rev. B **87**(8), 085442 (2013).
16. W. S. Whitney, V. W. Brar, Y. Ou, Y. Shao, A. R. Davoyan, D. N. Basov, K. He, Q. K. Xue, and H. A. Atwater, "Gate-variable mid-infrared optical transitions in a (bi1-xsbx)2te3 topological insulator," Nano Lett. **17**(1), 255–260 (2017).
17. J. Yin, H. N. S. Krishnamoorthy, G. Adamo, A. M. Dubrovkin, Y. Chong, N. I. Zheludev, and C. Soci, "Plasmonics of topological insulators at optical frequencies," NPG Asia Mater. **9**(8), e425 (2017).
18. M. Zhao, J. Zhang, N. Gao, P. Song, M. Bosman, B. Peng, B. Sun, C.-W. Qiu, Q.-H. Xu, Q. Bao, and K. P. Loh, "Actively tunable visible surface plasmons in bi2te3and their energy-harvesting applications," Adv. Mater. **28**(16), 3138–3144 (2016).
19. J. Toudert and R. Serna, "Interband transitions in semi-metals, semiconductors, and topological insulators: A new driving force for plasmonics and nanophotonics [invited]," Opt. Mater. Express **7**(7), 2299 (2017).
20. J. Y. Ou, J. K. So, G. Adamo, A. Sulaev, L. Wang, and N. I. Zheludev, "Ultraviolet and visible range plasmonics in the topological insulator Bi1.5Sb0.5Te1.8Se1.2," Nat. Commun. **5**(1), 5139 (2014).
21. B.-L. Huang and M. Kaviany, "Ab initio and molecular dynamics predictions for electron and phonon transport in bismuth telluride," Phys. Rev. B **77**, 125209 (2008).
22. D. Hsieh, Y. Xia, D. Qian, L. Wray, F. Meier, J. H. Dil, J. Osterwalder, L. Patthey, A. V. Fedorov, H. Lin, A. Bansil, D. Grauer, Y. S. Hor, R. J. Cava, and M. Z. Hasan, "Observation of time-reversal-protected single-dirac-cone topological-insulator states in Bi2Te3 and Sb2Te3," Phys. Rev. Lett. **103**(14), 146401 (2009).
23. B. Dastmalchi, P. Tassin, T. Koschny, and C. M. Soukoulis, "A new perspective on plasmonics: Confinement and propagation length of surface plasmons for different materials and geometries," Adv. Opt. Mater. **4**(1), 177–184 (2016).
24. P. B. Johnson and R. W. Christy, "Optical constants of the noble metals," Phys. Rev. B **6**(12), 4370–4379 (1972).
25. W. S. M. Werner, K. Glantschnig, and C. Ambrosch-Draxl, "Optical constants and inelastic electron-scattering data for 17 elemental metals," J. Phys. Chem. Ref. Data **38**(4), 1013–1092 (2009).
26. K. M. McPeak, S. V. Jayanti, S. J. Kress, S. Meyer, S. Iotti, A. Rossinelli, and D. J. Norris, "Plasmonic films can easily be better: Rules and recipes," ACS Photonics **2**(3), 326–333 (2015).
27. G. V. Naik, J. L. Schroeder, X. Ni, A. V. Kildishev, T. D. Sands, and A. Boltasseva, "Titanium nitride as a plasmonic material for visible and near-infrared wavelengths," Opt. Mater. Express **2**(4), 478–489 (2012).
28. S. J. Kim, P. Fan, J.-H. Kang, and M. L. Brongersma, "Creating semiconductor metafilms with designer absorption spectra," Nat. Commun. **6**(1), 7591 (2015).
29. B. Gholipour, G. Adamo, D. Cortecchia, H. N. S. Krishnamoorthy, M. D. Birowosuto, N. I. Zheludev, and C. Soci, "Organometallic perovskite metasurfaces," Adv. Mater. **29**(9), 1604268 (2017).
30. S. Guerin and B. E. Hayden, "Physical vapor deposition method for the high-throughput synthesis of solid-state material libraries," J. Comb. Chem. **8**(1), 66–73 (2006).
31. D. H. Kim, E. Byon, G. H. Lee, and S. Cho, "Effect of deposition temperature on the structural and thermoelectric properties of bismuth telluride thin films grown by co-sputtering," Thin Solid Films **510**(1-2), 148–153 (2006).
32. S. Lee, K. Esfarjani, T. Luo, J. Zhou, Z. Tian, and G. Chen, "Resonant bonding leads to low lattice thermal conductivity," Nat. Commun. **5**(1), 3525 (2014).
33. N. Han, S. I. Kim, J. D. Yang, K. Lee, H. Sohn, H. M. So, C. W. Ahn, and K. H. Yoo, "Phase-change memory in Bi_2Te_3 nanowires," Adv. Mater. **23**(16), 1871–1875 (2011).

Plasmonic nanostructures, including photonic metamaterials, have conventionally been fabricated from noble metals such as gold and silver [1]. The drawbacks of these metals in relation to certain applications (e.g. high Ohmic losses, abundance, cost) are well documented [2–5] and have inspired a search for alternative material platforms that encompasses conductive oxides, nitrides, superconductors, graphene and other 2D materials, to name but a few. The infrared plasmonic properties of conductive oxides (such as zinc oxide - AZO) can be controlled by doping [6–8] but otherwise, as singular elemental or stoichiometrically fixed crystalline compounds, these platforms present no possibility for controlled engineering or active switching of electromagnetic response parameters. In contrast, chalcogenide semiconductors – alloys containing at least one of the chalcogen (periodic table group 16) elements sulfur, selenium or tellurium – are well-known for the compositional variety of their

Optics EXPRESS

optical and electronic properties, and as phase-change media that can be switched in non-volatile fashion between physical states with markedly different refractive indices, conductivities, etc [9–14]. Certain crystalline chalcogenides (e.g. melt-grown Bi:Sb:Te:Se [15], chemically grown BiTe and epitaxial $(Bi_{1-x}Sb_x)_2Te_3$ [16–19]) have been demonstrated recently as topological insulators with low-loss metallic (plasmonic) surface states arising though strong spin-orbit interactions [20]. Here we show that amorphous, vapor-deposited (CMOS-compatible) thin films of bismuth telluride (Bi:Te) exhibit a plasmonic response at near-ultraviolet to visible frequencies, with the real part ε_1 of its relative permittivity taking a negative values over a composition-dependent range of wavelengths extending from as low as 250 nm to as high as 978 nm.

Bismuth telluride is widely known as an excellent thermoelectric material, possessing a narrow band gap, high density of states near the band edges and low thermal conductivity [21]. It has attracted renewed interest since its discovery as a 3D topological insulator [22], and in the form of chemically grown crystalline nanoplates has been observed to support surface plasmon modes in the visible wavelength range [18]. Its UV/VIS plasmonic response is demonstrated here in the first instance by variable angle spectroscopic ellipsometry measurements of relative permittivity (ε), such as presented in Fig. 1(a): the real part (ε_1) takes a negative value, as is required to support surface plasmons at an interface with a dielectric, between wavelengths λ_1 and λ_2 at which it is equal to zero (250 and 660 nm respectively in the example shown – a composition of 34% Bi and 66% Te, evaluated by energy-dispersive x-ray spectroscopy). Figure 1(b) presents the plasmonic figure of merit $FOM = Re\{k_{SPP}\}/2\pi Im\{k_{SPP}\}$ – effectively the surface plasmon polartiton (SPP) propagation decay length in units of SPP wavelength [17, 23] – for amorphous Bi:Te alongside a number of other, noble metal and a recently-proposed alternative plasmonic media [4]. ($k_{SPP} = k_0\sqrt{\varepsilon_m\varepsilon_d/(\varepsilon_m+\varepsilon_d)}$ being the wavevector of SPPs on a planar interface between metallic and dielectric media with complex relative permittivities ε_m and ε_d respectively; the latter is taken to be air in the present case; k_0 is the free space wavevector.) Bi:Te cannot match the plasmonic FOM of aluminum or silver at visible wavelengths (though Fig. 1(b) ignores the fact that their surfaces will oxidize/tarnish in air), but its FOM is higher than that of titanium nitride across the entire visible range (TiN being plasmonic only down to 500 nm), and higher than that of gold from 550 down to 350 nm.

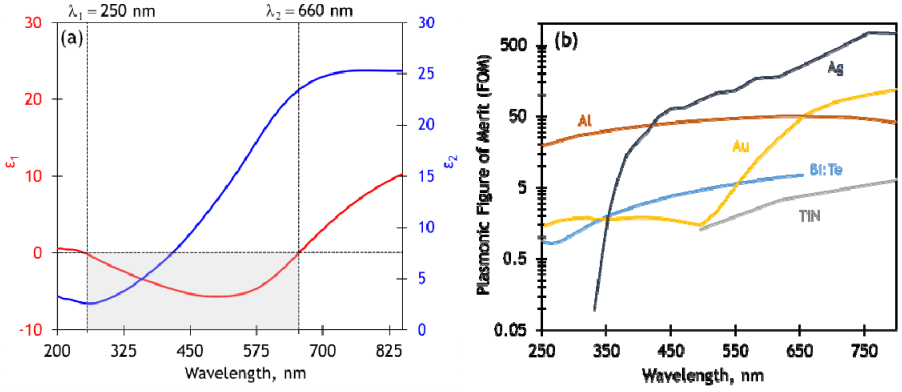

Fig. 1. Ultraviolet and visible plasmonics in amorphous Bi:Te. (a) Spectral dispersion of the relative permittivity of as-deposited amorphous bismuth telluride evaluated by variable angle spectroscopic ellipsometry for a 134 nm thick film of Bi[34%]:Te[66%] on a sapphire substrate. (b) Spectral dispersion of plasmonic figure of merit for amorphous as-deposited Bi(34%):Te(66%) and a selection of other plasmonic materials - as labelled; calculated using material parameters from Refs [24–27].

Optics EXPRESS

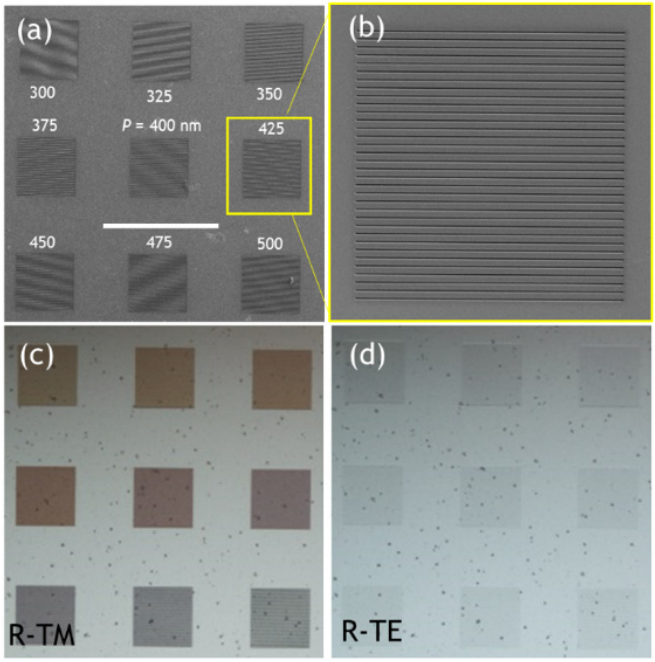

Fig. 2. Amorphous bismuth telluride metasurfaces. (a, b) Scanning electron microscopy images of nano-grating metasurfaces in 134 nm Bi[34%]:Te[66%] with periods ranging from 300 – 500 nm [as labelled; scale bar in (a) = 40 μm]. (c, d) Corresponding reflection mode optical microscopy images for (c) TM and (d) TE polarized incident light.

The plasmonic character of amorphous Bi:Te is demonstrated through the fabrication of planar metasurfaces presenting absorption resonances in the visible range, specifically sub-wavelength period (i.e. non-diffractive) grating structures akin to those recently proposed for applications such as active nanophotonics photodetectors [28] and color-tunable photovoltaics [29]. Optically thick (transmission <1%) Bi:Te films were deposited on optically flat sapphire substrates (pre-baked at 150°C for 30 minutes) by co-evaporation from elemental sources of ≥99.9999% purity. A base pressure of 1.7×10^{-8} mbar was achieved prior to deposition and the substrate was held within 10 K of room temperature on a water-cooled platen ~15 cm from the sources to produce low-stress amorphous films [30]. Film thickness is measured using a stylus profilometer. Nano-grating metasurface patterns, with a fixed linewidth L~100 nm and periods P ranging from 300 to 500 nm, each covering an area of approximately 20 μm × 20 μm, were etched through the Bi[34%]:Te[66%] layer by focused ion beam (FIB) milling [29].

Normal-incidence optical characteristics of the Bi:Te nano-grating metasurfaces were subsequently quantified using a microspectrophotometer (CRAIC QDI2010) with a sampling domain size of 15 μm × 15 μm, for incident polarizations parallel and perpendicular to the grating lines (TE and TM orientations of the grating respectively, as indicated in the inset to Fig. 3(a)). Unstructured amorphous Bi:Te has spectrally near-flat reflectivity of ~50% across the near-UV to near-IR spectral range, as shown in Fig. 3(a). Nano-grating metasurface structures introduce plasmonic resonances for TM polarized light (incident electric field perpendicular to the grating lines) which manifest themselves as period-dependent 'structural colors' [as illustrated in Fig. 2(c)], while no resonances are observed for TE polarized light – indeed, under TE illumination the nano-grating domains are almost indistinguishable from unstructured Bi:Te [Fig. 2(d)].

Optics EXPRESS

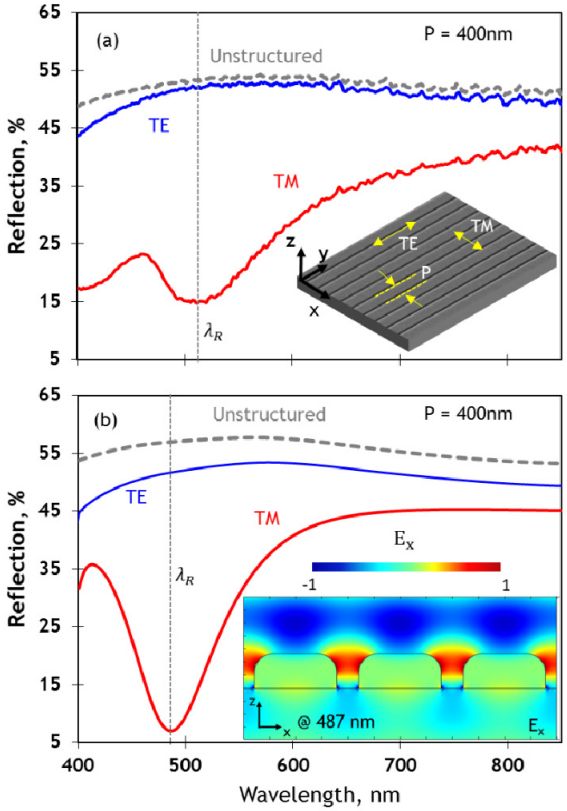

Fig. 3. Optical response of amorphous Bi:Te nano-grating metasurface. (a) Measured spectral dispersion of normal incidence reflectivity for a 400 nm period amorphous Bi[34%]:Te[66%] nano-grating metasurface for TM and TE-polarized incident light, and the corresponding (polarization-independent) spectrum for unstructured Bi:Te. The inset schematic illustrates TM/TE polarization orientations and coordinate axes as used in numerical simulations. (b) Numerically simulated spectral dispersion of normal incidence reflectivity related to the corresponding experimental spectra shown in panel (a). The inset presents the numerically simulated distribution of the *x*-component of electric field in the *xz* plane at the 487 nm TM resonance wavelength of the P = 400 nm nano-grating metasurface.

The nature of the TM resonance is illustrated via 3D finite element (Comsol MultiPhysics) numerical simulations, employing ellipsometrically measured material parameters for Bi:Te [Fig. 1(a)]. They assume normally incident narrowband plane wave illumination in the $-z$ direction of Bi:Te gratings in free space and, by virtue of periodic boundary conditions, structures of infinite extent in the xy plane. The TM plasmonic resonance is characterized by a local enhancement of field in the milled slots of the nano-grating structure [Fig. 3(b), inset]. The small spectral offset between measured and numerically simulated resonance (reflection minimum) wavelengths λ_R is ascribed primarily to the fact that experimental data is obtained with a focused microspectrophotometer probe beam as opposed to the (computationally assumed) normally incident plane wave. In contrast, there is no localization or enhancement of field under TE illumination. The spectral tuning of TM resonance wavelength with nano-grating period, shown in Fig. 4(a), is accurately reproduced by the computational model [Fig. 4(b)], with minor discrepancies between experiment and simulation being attributed to manufacturing imperfections and inhomogeneity (deviations from the ideal model geometry, such as slight over-milling of grating lines into the substrate) and some implantation of gallium into the Bi:Te during FIB milling, likely to effect a small change in refractive index.

Optics EXPRESS

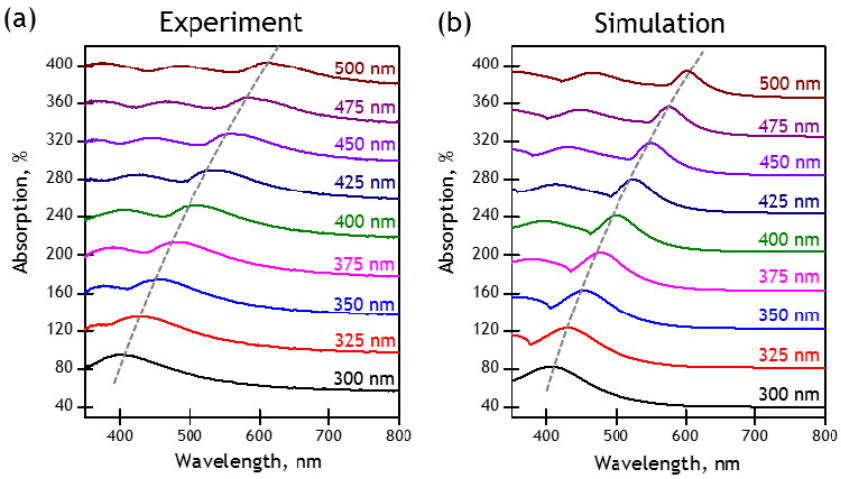

Fig. 4. Structural tuning of amorphous Bi:Te metasurface resonance wavelength. (a) Measured and (b) numerically simulated spectral dispersion of Bi[34%]:Te[66%] nano-grating metasurface TM-mode absorption for grating periods P ranging from 300 to 500 nm [as labelled; vertically offset in 40% steps for clarity; Numerical spectra are evaluated for an off-normal incident angle of 9°, as opposed to normal incidence, to more realistically represent the focused probe beam produced by the microspectrophotometer's objective lens].

Thus far we have considered a single Bi:Te compositional ratio of 34% Bi to 66% Te. Varying composition though has a profound effect on the optical properties of the alloy, providing an effective means of controlling the wavelengths at which $\varepsilon_1 = 0$, and therefore the spectral band over which the material is plasmonic (i.e. has a negative value of ε_1), as well as the corresponding losses (ε_2). By employing "wedge shutters" which partially shadow the elemental deposition sources [29], spatial compositional gradients of Bi and Te, thin film samples are produced in which the Bi:Te at% ratio varies continuously as a function of position over the substrate, from 1.6 to 17. This high-throughput approach enables rapid, systematic mapping of material parameters, i.e. complex relative permittivity, measured by variable-angle spectroscopic ellipsometry as a function of position, to composition [Fig. 5(a) and 5(b)]. While the near-UV ε_1 zero-crossing wavelength λ_1 and losses at this point are found to be largely invariant as a function of alloy composition, the longer zero-crossing wavelength λ_2, and associated losses are strong functions of the compositional ratio [Fig. 5(c) and 5(d)]: λ_2 red-shifts as the ratio increases, i.e. as the proportion of bismuth increases. In the present case it is tuned from 530 nm at a Bi:Te ratio of 0.06 to 978 nm at 0.60. As such the width of the alloy's plasmonic band increases with compositional ratio [Fig. 5(c)] to encompass the entire visible spectral range at higher Bi:Te ratios, though losses (ε_2) at longer wavelengths also increase with said ratio [Fig. 5(d)].

In summary, using high-throughput physical vapor deposition and characterization techniques, we demonstrate that amorphous bismuth telluride can serve as a composition-dependent material platform for UV/VIS plasmonics. The plasmonic character of the chalcogenide is illustrated via the fabrication of subwavelength period nano-grating metasurfaces, which present a highly anisotropic optical response: Under TM-polarized illumination (incident electric field perpendicular to the grating lines) plasmonic absorption resonances are manifested as period-dependent variations in the perceived color of the nanostructured domains, while for TE-polarized light the metasurface domains are almost indistinguishable from unstructured Bi:Te.

Optics EXPRESS

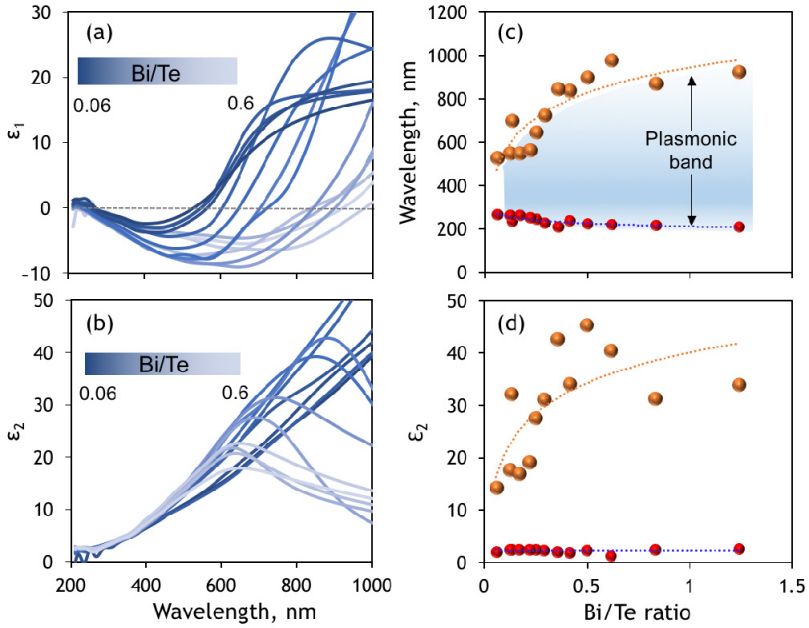

Fig. 5. Compositional tuning of Bi:Te optical properties. (a, b) Spectral dispersion of the (a) real and (b) imaginary parts of relative permittivity for as-deposited amorphous bismuth telluride across a range of Bi:Te at% compositional ratios, evaluated via variable angle spectroscopic ellipsometry. (c, d) Dependence on Bi:Te ratio of (c) the wavelengths at which the real part of relative permittivity $\varepsilon_1 = 0$, and (d) corresponding values of ε_2. Red dots refer to the shorter wavelengths crossover point while orange dots refer to the longer wavelengths crossover point.

Bismuth telluride offers a uniquely adaptable, material base for plasmonics and nanophotonics with compositionally controlled optical properties. While presenting a plasmonic response in an as-deposited amorphous thin film that holds a significant advantage over bulk and solution-processed crystalline chalcogenides (and various other 'alternative plasmonic' media) in terms of device production process compatibility and scalability. Alongside established credentials as a thermoelectric medium [31], and the possibility of non-volatile electrically/optically-induced phase-change switching of properties [32, 33], it presents intriguing possibilities for the control of photons and electrons in thin film thermo/opto-electronics, including for aesthetic purposes (e.g. harnessing plasmonic 'structural color' in building-integrated thermoelectric devices). Furthermore, the high throughput approach to compositional tuning used in this study can be extended beyond binary alloys to ternary or doped ternary chalcogenides with the possibility of combining different physical properties (phase change, magnetic, electrical) with the mapped optical properties opening up the possibility of optimizing composition for a variety of different device applications.

Funding

UK Engineering and Physical Sciences Research Council [grant EP/M009122/1] and the Ministry of Education, Singapore [grant MOE2016-T3-1-006].

Acknowledgments

The data from this paper can be obtained from the University of Southampton ePrints research repository: https://doi.org/10.5258/SOTON/D0437.